C Cowley, A Q Kuang, D Moulton, J D Lore, J Canik,
M Umansky, M Wigram, S Ballinger, B Lipschultz

Novel SOLPS-ITER Simulations of X-point target and Snowflake Divertors

Novel SOLPS-ITER Simulations of X-point target and Snowflake Divertors

C Cowley, A Q Kuang, D Moulton, J D Lore, J Canik, M Umansky,

M Wigram, S Ballinger, B Lipschultz

Novel SOLPS-ITER Simulations of X-point target and Snowflake Divertors

C Cowley[1,3]**, A Q Kuang**[2]**, D Moulton**[3]**, J D Lore**[4]**, J Canik**[4]**, M Umansky**[5]**, M Wigram**[2]**, S Ballinger**[2]**, B Lipschultz**[1]** and X Bonnin** [6]

[1] York Plasma Institute, University of York, Heslington, York, YO10 5DQ, UK

[2] MIT Plasma Science and Fusion Center, 167 Albany St, Cambridge, MA 02139, United States

[3] UKAEA-CCFE, Culham Science Centre, Abingdon, OX14 3DB, UK

[4] Oak Ridge National Laboratory, 5200, 1 Bethel Valley Rd, Oak Ridge, TN 37830, United States

[5] Lawrence Livermore National Laboratory, 7000 East Ave., Livermore CA 94550

[6] ITER Organization, Route de Vinon-sur-Verdon, CS 90 046, 13067, St. Paul Lez Durance Cedex, France

E-mail: czlc500@york.ac.uk

Abstract.

The design and understanding of alternative divertor configurations may be crucial for achieving acceptable steady-state heat and particle material loads for magnetic confinement fusion reactors. Multiple x-point alternative divertor geometries such as Snowflakes and X-point targets have great potential in reducing power loads, but have not yet been simulated widely in codes with kinetic neutrals. This paper discusses recent changes made to the SOLPS-ITER code to allow for the simulation of X-point target and low-field side snowflake divertor geometries. Snowflake simulations using this method are presented, in addition to the first SOLPS-ITER simulation of the X-point target. Analysis of these results show reasonable consistency with the simple modelling and theoretical predictions, supporting the validity of the methodology implemented.

1. Introduction

Maintaining manageable heat and particle loads on materials presents a significant challenge to overcome for high power magnetic confinement fusion reactors. For reactor-like machines such as ITER and SPARC [1], empirical scalings predict deposited target heat loads in excess of $25\mathrm{MWm}^{-2}$ [2, 3]; significantly higher than the $\approx 15\ \mathrm{MWm}^{-2}$ steady-state surface heat load limit on tungsten monoblock tiles [4]. Additionally, the high loads of energetic particles in these machines can lead to erosion rates of more than $15\mathrm{nm\ s}^{-1}$ [2] on tungsten tiles, limiting the effective lifetime of these tiles and requiring more frequent, costly replacement of the divertor components. As a consequence, methods of reducing heat and particle loads in the divertor will be important for operating future devices; methods such as injecting radiating impurities and operating with alternative divertors.

Alternative divertors are divertors which leverage novel magnetic or geometric features differing from the 'standard' divertor; features which are predicted to benefit divertor exhaust in some way. One such alternative divertor is the Snowflake, which implements additional nulls near primary X-point, creating a higher order X-point, which has been shown to significantly increase divertor connection lengths [5] and may enhance cross-field transport through churning modes [6]. The X-point target (XPT) is another alternative divertor, which has a secondary X-point near the divertor targets [7]. The low poloidal field near this secondary X-point can lead to longer connection lengths, and there can be significant power sharing between the multiple outer divertor targets - depending on the X-point separation and strength of cross-field transport [8, 9]. Furthermore, the secondary X-point can be located at higher major radius than the primary, creating a magnetic flux expansion and lowering heat flux densities at the targets (similar to the Super-X divertor configuration [10]). Finally, the low poloidal field and local minimum in total field created by the secondary X-point could aid in detachment control [11, 12].

Despite the potential of Snowflake and XPT divertors, neither geometry has been widely simulated in codes with kinetic neutrals, particularly in the simulation code SOLPS-ITER [13, 14]. In fact, though snowflakes have been simulated in codes such as EMC3-EIRENE

[15, 16, 17], they have only been simulated once before in SOLPS-ITER [18], and XPTs have never been simulated previously using the code due to the rigidity of the physics modules and grid generators [14]. The benefits of using SOLPS-ITER include the complex kinetic treatment of neutrals through its coupling to the EIRENE Monte-Carlo solver, the ability to activate drifts and currents, and the extensive history and benchmarking of the code [14]. In this work we propose a new generalised method for simulating both X-point target and low-field side snowflake divertors within SOLPS-ITER, which may allow more widespread simulation of these alternative geometries; furthering the understanding of such divertors. Building on work performed in [18], the modifications to SOLPS-ITER have been generalized and can be integrated with the rest of the code with no loss of functionality for standard grids.

2. Methodology

When running a SOLPS-ITER simulation of a new geometry, it is first necessary to generate relevant input files. This is typically done using a combination of the DivGeo software for basic input specification, the standard grid builder CARRE [19], and other preprocessing routines. After generating the relevant input files, the physics simulations can be run, which for SOLPS-ITER is typically a coupled simulation of the fluid solver B2.5 and the kinetic Monte Carlo code EIRENE [20].

However, previous versions of SOLPS-ITER only work for an expected list of geometries, including single null divertors, double null divertors, slab geometries, annular geometries, limited geometries and stellarator islands. For more unconventional grids such as the XPT, there are two main issues that prevent using this standard workflow. First, the physics modules of SOLPS-ITER expect a double null geometry if a grid is given that contains two X-points. The second issue is that the grid builder CARRE is unable to build grids using equilibria with two X-points connected to the same O-point.

Consequently, to run a SOLPS-ITER simulation of a Snowflake or XPT requires solutions to these two issues. Solutions to these challenges have been developed throughout this work and will be presented in the following section.

2.1. Modifying SOLPS-ITER Source

The first challenge to be solved before XPT or Snowflakes can be simulated in SOLPS-ITER is the fact that the fundamental physics modules are not expecting such geometries. Instead, when two X-points are detected in the geometry, SOLPS-ITER assumes the grid is a double null. These assumptions are present because the B2.5 plasma grid must be rectangular when mapped into poloidal and radial index coordinates.The introduction of X-points or more than two targets introduces 'cuts' into the grid, where the poloidal neighbor of a cell is not the cell that is adjacent in physical space. To prepare the geometry correctly, SOLPS-ITER assumes a certain order of X-point and target cuts. If two disconnected X-points are detected, the

code assumes the ordering is that of a disconnected double null (DDN), which is shown in Figure 1.
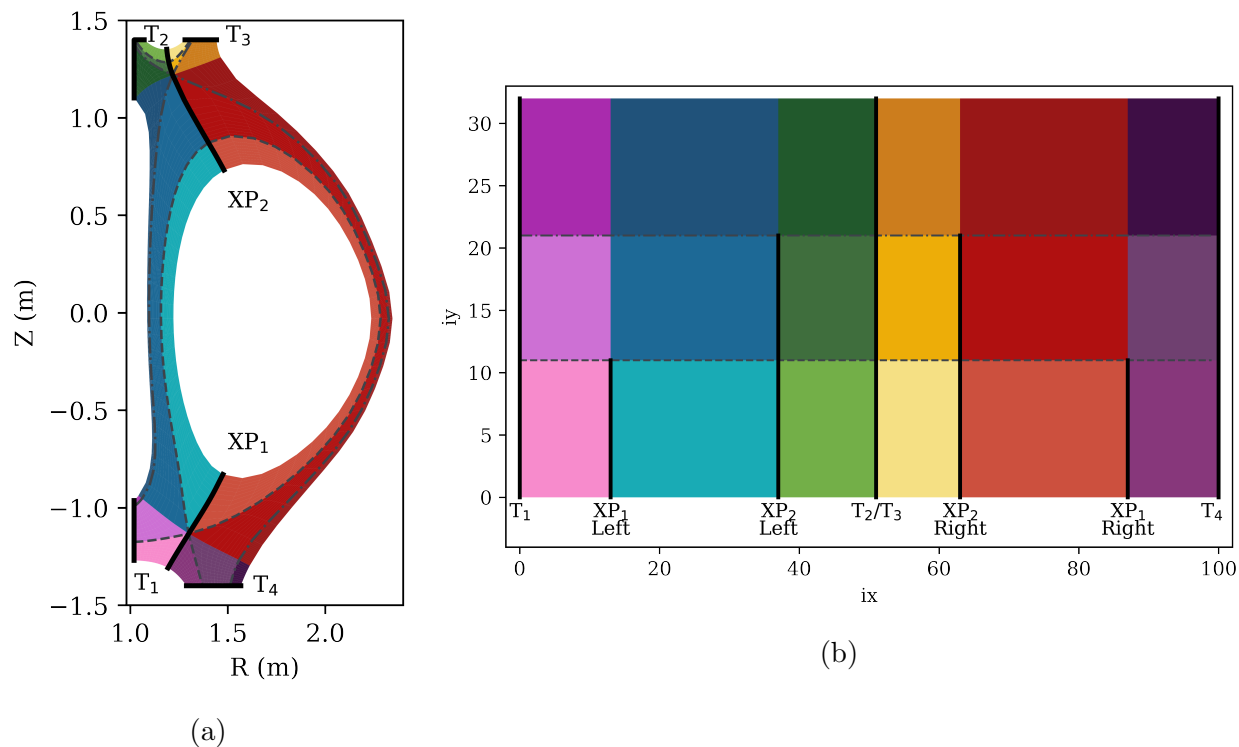

(a)

(b)

Figure 1: The patch diagrams of a disconnected double null divertor mapped in a) physical coordinates and b) poloidal (ix) and radial (iy) index coordinates.
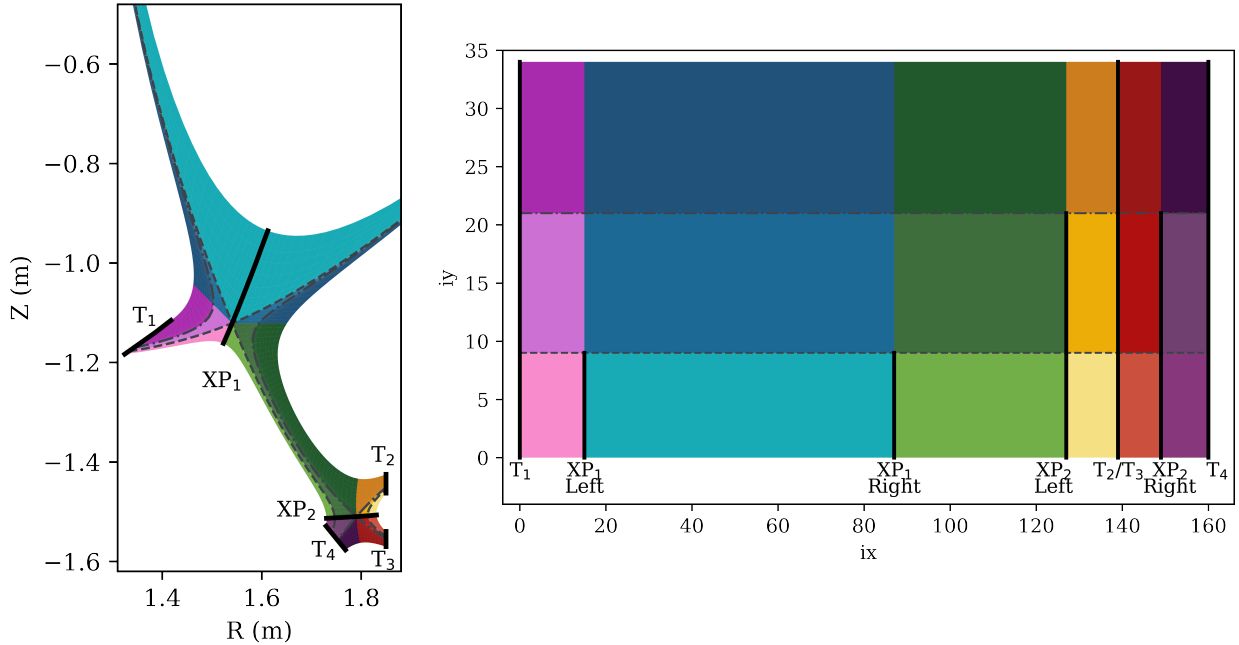
Figure 2: The patch diagrams of a lower X-point target divertor mapped in a) physical coordinates and b) poloidal (ix) and radial (iy) index coordinates.

Figure 2 on the other hand shows the geometry of a lower XPT and its rectangular mapping, which is similar to a snowflake minus with the secondary X-point on the low-field side. A low-field side snowflake plus is poloidally similar as well, but with different radial region definitions. From Figures 1 and 2, one can see that the DDN and XPT geometries are similar, with three radial regions, four cuts due to X-points, and one cut due to intermediate targets. However, the figure also shows that the ordering of these cuts is subtly but crucially different. In the DDN case the target cut is the 3rd cut to be encountered poloidally, whereas in the XPT case the intermediate targets comprise the 4th poloidal cut. Moreover, if we label the primary X-point as 1, and the secondary as 2, then in order of increasing in poloidal index the DDN encounters 1,2,2,1; contrarily, the XPT encounters 1,1,2,2.

Because the ordering of XPT cuts are different from what SOLPS-ITER expects, a standard run of the code will fail if an X-point target or Snowflake grid is provided. To overcome this, several B2.5 preprocessing routines, and B2.5-EIRENE interfacing routines were edited to detect whether a grid has a DDN or an XPT (equivalently a low-field side Snowflake) ordering of primary and secondary X-point cuts. If a DDN is detected, the code will run in its unedited form, expecting the cut order shown in Figure 1. If an XPT or Snowflake is detected, however, new code has been written to unpack grid data according to an ordering of cuts shown in Figure 2. With this modified code, XPTs and low-field side snowflakes (both plus and minus) can be simulated without taking away from any previous SOLPS-ITER functionality. The code modifications have not yet been implemented to allow for a high-field side snowflake, though this could be achieved in much the same way.

2.2. Input File Generation

The second issue to overcome in simulating XPTs or snowflakes in SOLPS-ITER is the fact that relevant input files cannot be generated through the standard grid builder CARRE. As such, a custom workflow was developed to prepare the required input files for a SOLPS-ITER run without the use of CARRE. This workflow consists of three unique steps, followed by a continuation of the regular SOLPS-ITER workflow.

The first step in the custom XPT simulation workflow is similar to that of a regular workflow, in that it revolves around generating a basic input structure with the graphical user interface DivGeo. Plasma facing components (PFCs) are loaded into DivGeo and adjusted manually if necessary. The plasma species, wall material, and recycling coefficients are specified. The second step of this process is generating the XPT grid mesh from an equilibrium. To do this, we have used INGRID [21], a grid generator than can use snowflake and X-point target equilibria, among others.

After the grid data is generated from INGRID and the species and surface data is obtained from DivGeo, the third step is to manually convert the surface data obtained from DivGeo and grid data into SOLPS-ready input files using custom python routines. After this third step, all geometry-dependent input files should be generated, and the remaining input files such as b2ar.dat can be written manually according to a user's preference. The standard preprocessing routines can then be run, followed by submission of the simulation itself until convergence is achieved. Converged SOLPS-ITER simulations have been obtained for a snowflake-minus, snowflake-plus, and for the first time for an XPT geometry. The results of these geometries will be discussed over the following sections.

3. TCV-like Snowflake Minus Simulations

As part of the validation of this novel workflow, a snowflake plus geometry has been simulated in SOLPS-ITER. The equilibrium used is similar to that of TCV, though the PFCs are unique to this study. An input power and core density of 20 KW and 1.1×10^{19} m^{-3} were used, and the electron temperature profile of the converged solution is shown in Figure 3a. The profiles from this figure are well behaved, and in general this configuration is not greatly effected by the presence of the secondary x-point. This is not unexpected, since the two x-points have a large poloidal separation, and this equilibrium was simply chosen for demonstration purposes. Moreover, inspecting the plasma fluid velocity profile in Figure 3b, it is clear there is no unexpected or anomalous transport near the additional x-point boundaries.
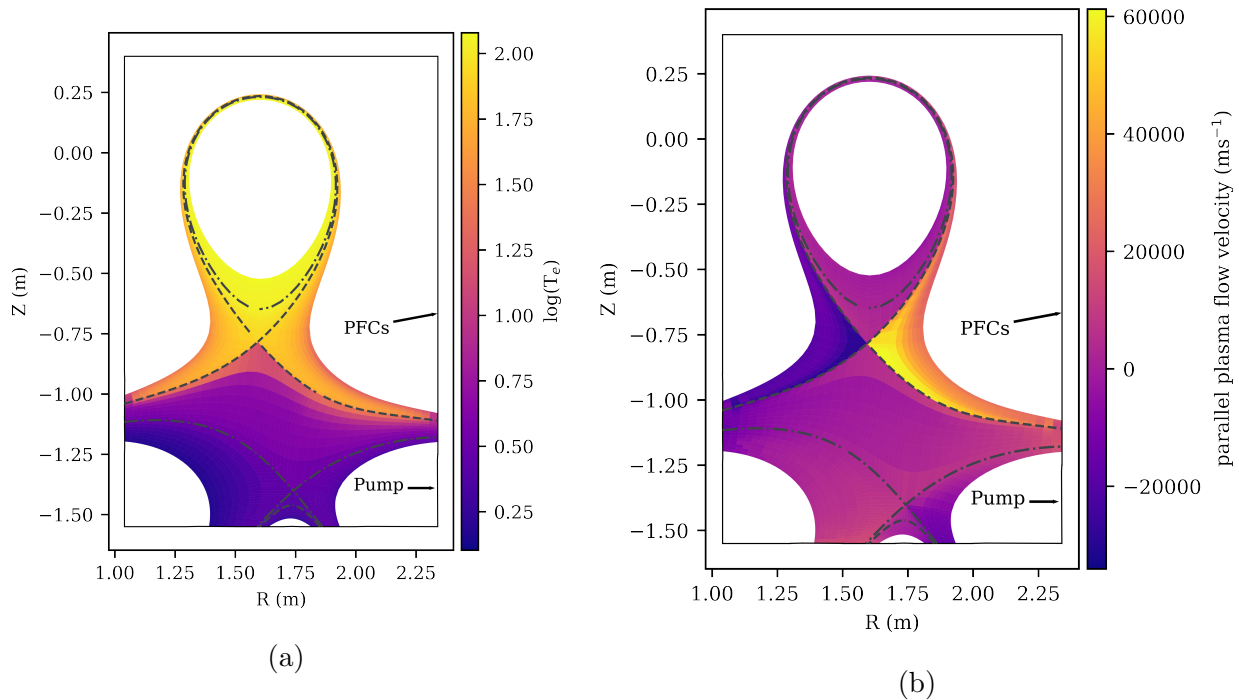
Figure 3: a) A logarithmic 2d electron temperature map of a converged SOLPS-ITER simulation of a TCV-like snowflake plus equilibrium. b) A 2d plot of plasma fluid velocity for the simulation in a).

4. SPARC-Like X-point Target Results

For this study a SPARC lower XPT geometry was simulated to verify the modified code and workflow. In this geometry the two separatrixes are 0.4mm apart mapped to the outer midplane, and the XPT simulation was compared to a lower single null (SN) with a similar plasma current. The XPT grid files were generated using the novel workflow in Section 2, whereas the SN input files were generated using the standard CARRE workflow as a benchmark for comparison. PFC contours for both simulations are based upon those of SPARC, but are modified to allow a wider simulation domain. When the relevant input files were obtained, both simulations were run with the same coupled SOLPS-ITER routines. Both grids were roughly matched in terms of radial boundaries; the single null extending from -7.4mm to +1.7mm from the separatrix at the outer midplane, and the XPT extending from -7.8mm to +2.0mm.

The SN and XPT simulations were pure deuterium simulations without drifts. The same input power of 200 kW and approximately the same outer midplane density of 1.15E19 m^{-3} were used for both simulations. Note that these values are not representative of SPARC, but have been used to access a regime of modest heat and particle flux (where extensive validation of SOLPS-ITER has been performed) without the need for impurities. The transport coefficients were also held constant for both runs, to achieve a ≈ 0.4 mm heat

flux fall off width at the X-point mapped to the midplane and a $\approx 4\text{mm}$ density fall off width at the outer midplane. Crucially, because no impurities are used and because both grids have similar total flux expansions, there should be little heat flux dissipation in both SN and XPT simulations. Moreover, the separation of the separatrixes is relatively large at $\approx 1\lambda_q$, so there shouldn't be significant modification of peak heat fluxes due to the secondary x-point. As such, the agreement of these simulations can serve as an effective benchmark for the new code changes and workflow.
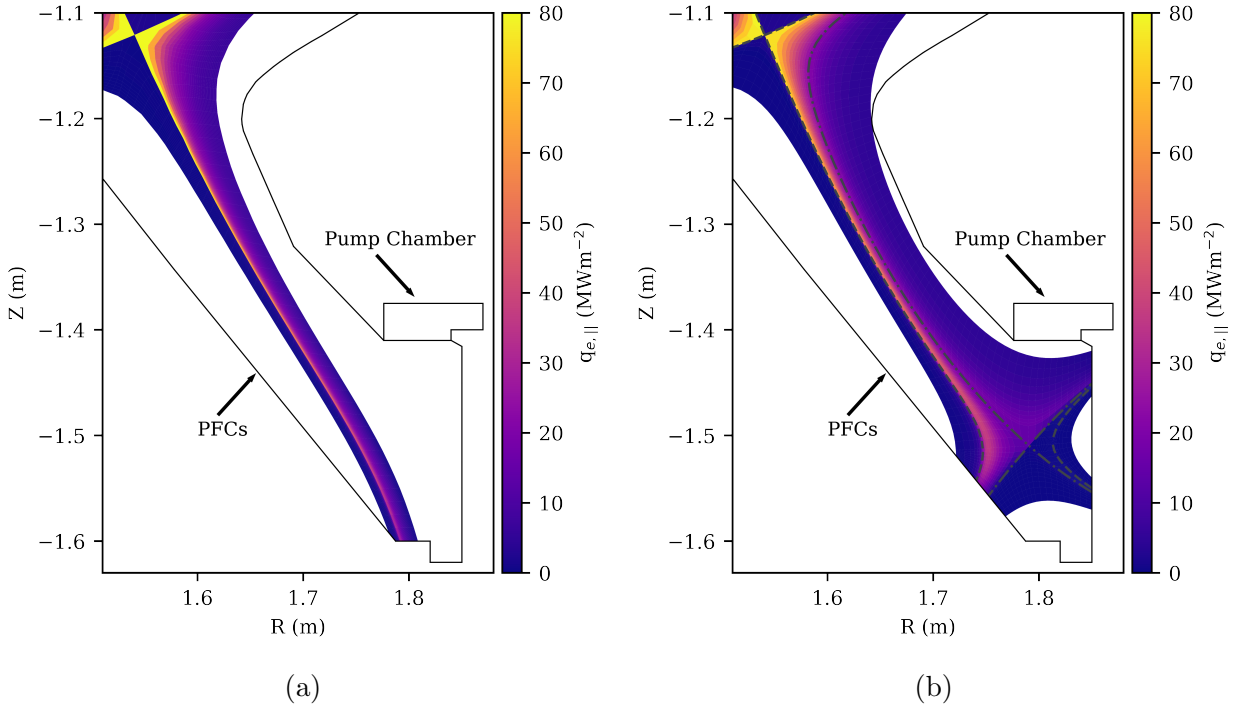

Figure 4: The 2D electron heat flux density profile of a a) SPARC SN and b) SPARC XPT SOLPS-ITER simulation. PFCs are shown in black.

The 2D parallel electron heat flux density profiles of the SN and XPT simulations are shown in Figures 4a and 4b respectively. From these figures, it is clear to see good overall qualitative agreement between the two grids, both in profile shape further upstream and the maximum and minimum heat flux values throughout the divertor. Furthermore, the radial profiles of the parallel heat flux density at the divertor entrance can be seen in Figure 5a, and also show good quantitative and qualitative agreement. In particular, both profiles show a peak parallel heat flux density of 80 MWm^{-2}, and a fall-off width of $\approx 0.4\text{mm}$.

Given that the upstream profiles of the two grids are similar, and that there are no strong heat dissipation mechanisms such as impurities, then the target parallel heat flux density profiles in the two cases should be similar. Indeed, the target parallel heat flux densities are plotted in Figure 5b, and show a similar qualitative profile between the single null and XPT grids. Moreover, when the target profiles for the two primary targets for the X-point target

are overlaid, they form one relatively continuous profile apart from at the secondary X-point at $\approx$ 0.4mm from the primary separatrix. This tends to support the idea that these physics simulations are running with no issues, and that the baseline grid is mapped correctly.
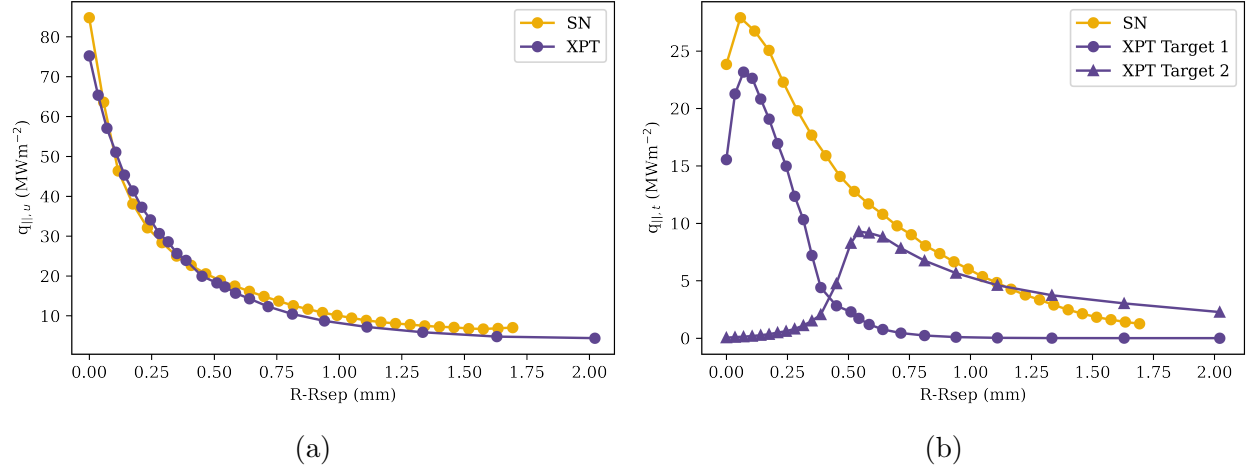

(a)

(b)

Figure 5: The target electron a) heat flux density and b) static pressure profiles as a function of radial distance from the separatrix (mapped to the outer midplane) for a SPARC single null and XPT divertor.
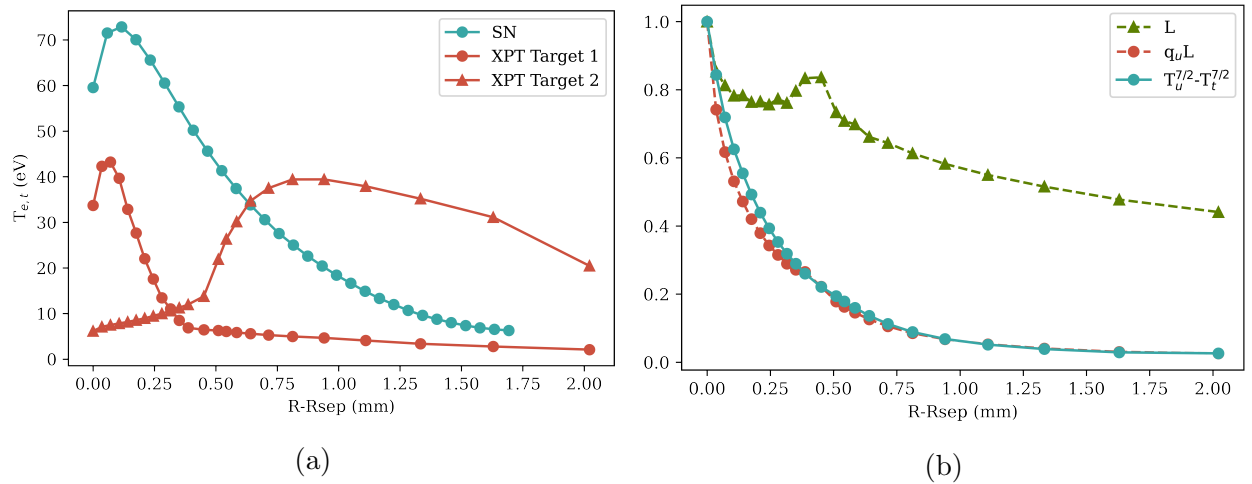

(a)

(b)

Figure 6: The target electron a) density and b) temperature profiles as a function of radial distance from the separatrix (mapped to the outer midplane) for a SPARC single null and XPT divertor.

Finally, the target electron temperature profiles for both simulations are plotted in Figure 6a. Unlike the heat flux profiles, these profiles differ significantly between the two grids. However, this is not unexpected given that ultimately the grids are not identical, and in fact the connection length profiles vary between the two. What is crucial to determine,

therefore, is whether these differences in target parameters can be explained by physics analysis. Using simple arguments of the two point model, the target temperature should vary [22]:

$$T_u^{7/2} - T_t^{7/2} = q_{||,u} L \kappa_1 \tag{1}$$

Where $L_{||}$ is the connection length and κ_1 is the Spitzer conductivity divided by $T^{5/2}$, which is typically taken approximated as a constant simple two point model analysis. Consequently, given a constant κ_1 and assuming the heat flux density does not change significantly over the divertor volume, the difference in upstream and downstream temperatures to the power 7/2 should vary with $q_{||,u} L_{||}$. The profiles of connection length, the product of connection length and heat flux density, and the difference in upstream and downstream temperatures to the power 7/2 are plotted in Figure 6b. Indeed, this figure shows the XPT simulation temperature profiles are in very good agreement with simple two point model physics. There is small deviation from the trend at R-R$_{sep}$ = 0.25mm, but this can be attributed to flux limited heat conduction and increased heat flux losses near the secondary separatrix.

5. MAST-U-like Snowflake Minus Results

The final simulations used for this study are of three MAST-U-like snowflake geometries. They are lower low-field side snowflake minus configurations, with various degrees of x-point separation, as can be seen in Figure 7. All three equilibria have been run with identical input powers and core boundary densities of 400KW and 1×10^{19} m^{-3}, along with identical transport coefficients. These equilibria have been used to verify the behavior of snowflakes as x-point separation is varied. One would expect that as the x-point separation increases, the ratio of power incident on the first and third outer target (shown in Figure 7) to change, with more power indecent on the third.
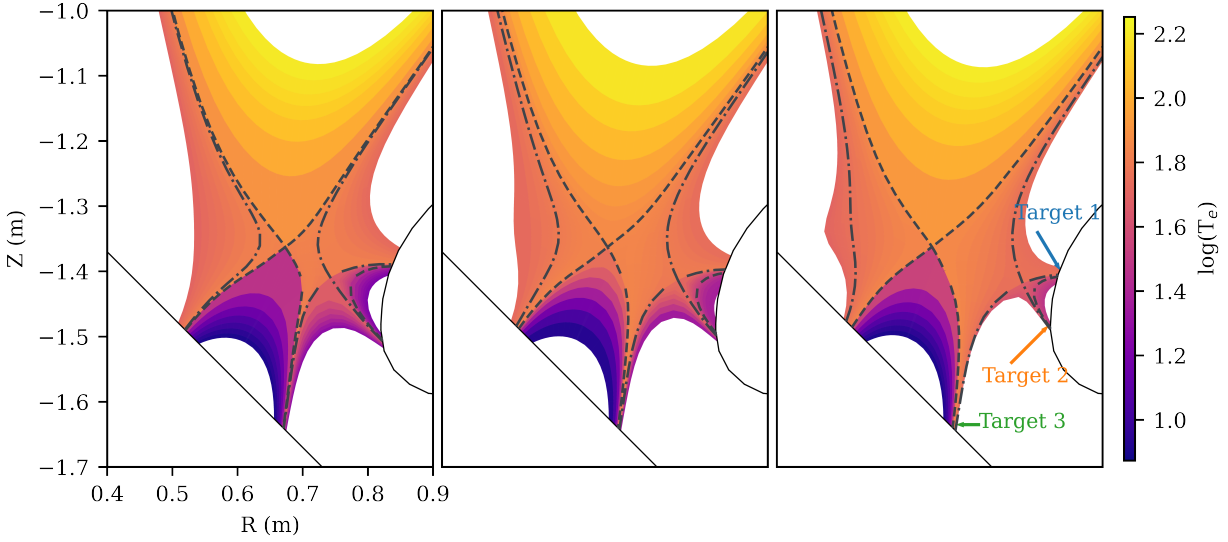
Figure 7: A 2d logarithmic plot of the electron temperature profiles of three MAST-U like snowflake simulations, with various x point separations.

To test these predictions, the fractional power load on each outer target has been plotted as a function of x-point separation for these grids, and is shown in Figure 8. The figure indeed shows consistency with expectations, as the fractional power to target 3 increases with x-point separation, whilst the target 1 power loading decreases. The second target receives very little power, which is expected given that it receives no parallel transport from the SOL, and any power loads must come from cross-field transport, neutral loading, or radiation.
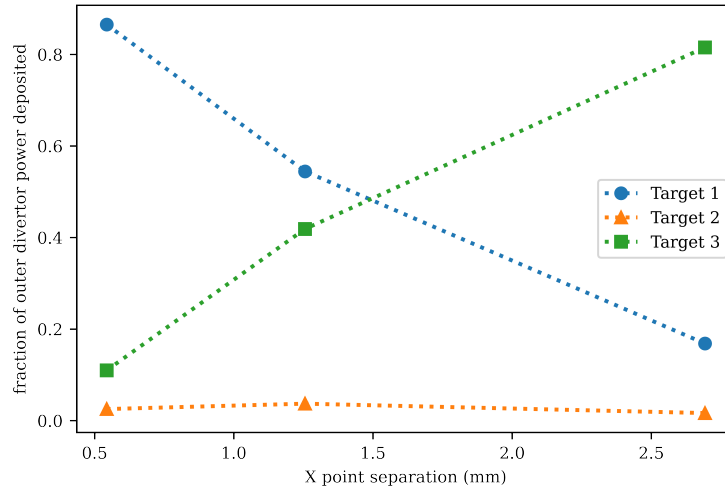

Figure 8: The electron temperature profiles of three MAST-U like snowflake simulations, with various x point separations.

Finally, when x-point separations are varied in a snowflake, it is important to understand

how the entire plasma state varies, not simply target loading. One important phenomena to study (and one which SOLPS-ITER lends itself to well) is how neutral transport can change with snowflake configuration. To this end, the EIRENE mesh neutral densities have been plotted for each simulation in Figure 7, and are shown in Figure 9. In these plots, the neutral density distribution changes as the peak in target ion flux changes from the first to the third target. In particular, the grid with the smallest x-point separation shows lower neutral density in the lower divertor chamber, and higher density in the SOL than the equilibria with larger separations. Though these simulations are not run with sputtered impurities, it is important to note that the separation of the x-points can also affect sputtered impurity content, as having too much sputtered impurities such as carbon in the upper SOL may negatively impact core performance and the pedestal.
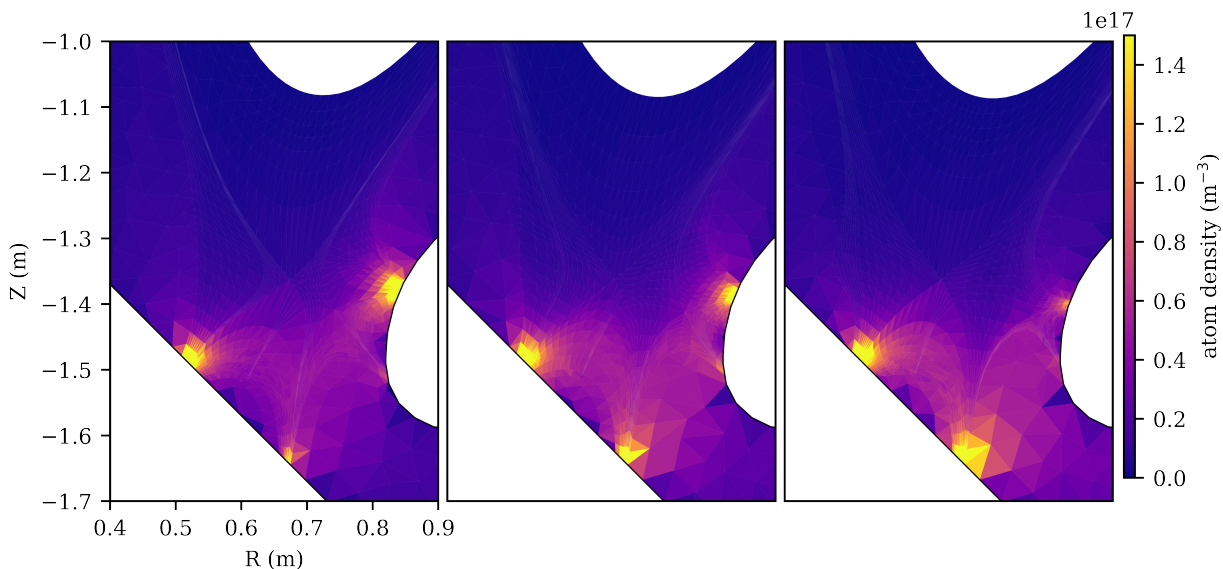

Figure 9: The 2d neutral density profiles of three MAST-U like snowflake simulations, with various x point separations.

6. Conclusions

Throughout this work, a new way of simulating X-point target and low-field side snowflake divertors in SOLPS-ITER is presented. The SOLPS-ITER source has been edited to accept multiple X-point alternative divertors, whilst still maintaining functionality for standard divertors. INGRID, an interactive python grid generator has been used to generate the grid data, which is then converted into SOLPS-ITER ready input files using custom python routines. Results and analysis from SOLPS-ITER simulation of a TCV-like snowflake plus, a SPARC-like X-point target, and MAST-U-Like snowflake minus equilibria have been presented, and demonstrate the robustness of the new workflow. Consistency of these simulations with predictions from the two-point model supports the validity of the results

presented. Moreover, the results show expected behavior when the x-point separation for a snowflake grid is varied. In future work this workflow should be used to leverage the full complexity of SOLPS-ITER, including drift-activated runs, and full multi-species transport.

7. Acknowledgments

References

[1] Creely AJ, Greenwald MJ, Ballinger SB, Brunner D, Canik J, Doody J, et al. Overview of the SPARC tokamak. Journal of Plasma Physics. 2020;86(5):865860502.

[2] Loarte A, Lipschultz B, Kukushkin A, Matthews G, Stangeby P, Asakura N, et al. Power and particle control. Nuclear Fusion. 2007;47(6):S203.

[3] Kuang AQ, Ballinger S, Brunner D, Canik J, Creely AJ, Gray T, et al. Divertor heat flux challenge and mitigation in SPARC. Journal of Plasma Physics. 2020;86(5):865860505.

[4] Pitts R, Bonnin X, Escourbiac F, Frerichs H, Gunn J, Hirai T, et al. Physics basis for the first ITER tungsten divertor. Nuclear Materials and Energy. 2019;20:100696.

[5] Ryutov D. Geometrical properties of a "snowflake" divertor. Physics of Plasmas. 2007;14(6):064502.

[6] Ryutov D, Cohen R, Rognlien T, Umansky M. A snowflake divertor: a possible solution to the power exhaust problem for tokamaks. Plasma Physics and Controlled Fusion. 2012;54(12):124050.

[7] LaBombard B, Marmar E, Irby J, Terry J, Vieira R, Wallace G, et al. ADX: a high field, high power density, advanced divertor and RF tokamak. Nuclear Fusion. 2015;55(5):053020.

[8] Wigram MRK, LaBombard B, Umansky M, Kuang A, Golfinopoulos T, Terry J, et al. Performance assessment of long-legged tightly-baffled divertor geometries in the ARC reactor concept. Nuclear fusion. 2019;59(10):106052.

[9] Umansky M, Rensink M, Rognlien T, LaBombard B, Brunner D, Terry J, et al. Assessment of X-point target divertor configuration for power handling and detachment front control. Nuclear Materials and Energy. 2017;12:918-23.

[10] Valanju PM, Kotschenreuther M, Mahajan S, Canik J. Super-X divertors and high power density fusion devices. Physics of Plasmas. 2009;16(5):056110.

[11] Lipschultz B, Parra FI, Hutchinson IH. Sensitivity of detachment extent to magnetic configuration and external parameters. Nuclear Fusion. 2016;56(5):056007.

[12] Cowley C, Lipschultz B, Moulton D, Dudson B. Optimizing detachment control using the magnetic configuration of divertors. Nuclear Fusion. 2022;62(8):086046.

[13] Bonnin X, Dekeyser W, Pitts R, Coster D, Voskoboynikov S, Wiesen S. Presentation of the new SOLPS-ITER code package for tokamak plasma edge modelling. Plasma and Fusion Research. 2016;11:1403102-2.

[14] Wiesen S, Reiter D, Kotov V, Baelmans M, Dekeyser W, Kukushkin A, et al. The new SOLPS-ITER code package. Journal of nuclear materials. 2015;463:480-4.

[15] Lunt T, Canal G, Duval B, Feng Y, Labit B, McCarthy P, et al. Numerical study of potential heat flux mitigation effects in the TCV snowflake divertor. Plasma Physics and Controlled Fusion. 2016;58(4):045027.

[16] Pan O, Lunt T, Wischmeier M, Coster D, et al. SOLPS simulations of detachment in a snowflake configuration for the future upper divertor in ASDEX Upgrade. Plasma Physics and Controlled Fusion. 2018;60(8):085005.

[17] Mao R, Fedorczak N, Ciraolo G, Bufferand H, Marandet Y, Bucalossi J, et al. Impact of an alternative divertor configuration on plasma detachment: pure deuterium simulations using the SOLEDGE2D-EIRENE edge transport code for HL-2M scenarios. Nuclear Fusion. 2019;59(10):106019.

[18] Pan O, Lunt T, Wischmeier M, Coster D, Stroth U, et al. SOLPS-ITER modeling with activated drifts for a snowflake divertor in ASDEX Upgrade. Plasma Physics and Controlled Fusion. 2020;62(4):045005.

[19] Marchand R, Dumberry M. CARRE: a quasi-orthogonal mesh generator for 2D edge plasma modelling. Computer Physics Communications. 1996;96(2):232-46.

[20] Schneider R, et al. SOLPS 2-D edge calculation code. Contrib Plasma Phys. 2006;46:3-191.

[21] Garcia B, Umansky M, Watkins J, Guterl J, Izacard O. INGRID: an interactive grid generator for 2D edge plasma modeling. Computer Physics Communications. 2022;275:108316.

[22] Stangeby PC, et al. The plasma boundary of magnetic fusion devices. vol. 224. Institute of Physics Pub. Philadelphia, Pennsylvania; 2000.